Water vapor oxidation of ferritic 441 and austenitic 316L stainless steels at 1100 °C for short duration

Valentin Badin, Entela Diamanti, Pierre Forêt, Evelyne Darque-Ceretti

Available online at www.sciencedirect.com

ScienceDirect

Procedia Materials Science 9 (2015) 48 – 53

Procedia Materials Science

www.elsevier.com/locate/procedia

International Congress of Science and Technology of Metallurgy and Materials, SAM – CONAMET 2014

Water vapor oxidation of ferritic 441 and austenitic 316L stainless steels at 1100 °C for short duration

V.Badin[a], E. Diamanti[b], P. Forêt[b], E. Darque-Ceretti[a,*]

[a]*MINES ParisTech, PSL - Research University, CEMEF - Centre for material forming, CNRS UMR 7635 CS10207 rue Claude Daunesse 06904 Sophia Antipolis Cedex, France*

[b]*Linde AG, Carl-von-Linde-Str. 25, 85716 Unterschleissheim, Germany*

Abstract

A ferritic 441 and an austenitic 316L steels have been exposed to wet argon at 1100 °C. This study focus on the characterization of the oxide scales formed after different exposure times in the range of 2.5-20 min. Raman spectroscopy, XRD, SEM and XPS have been used. For all exposure times, 316L forms a breakaway type thick oxide scale (rupture of the pre-existing passivating film) with iron oxides on its outer part and a mix of spinels with Fe, Cr and Ni for its inner part. For lower water vapor partial pressure, iron oxides are constituted of wüstite. For higher water vapor partial pressure, iron oxides are constituted of a layer of hematite over a layer of magnetite slightly enriched in chromium. Due to strong oxidation condition, oxide scale is not always homogeneous and iron oxides spallation may occur. For 2.5 min of oxidation on 441, a very thin layer of protective chromium oxide is formed. For longer exposure time, an almost homogeneous and much thicker layer mainly consisting of Cr_2O_3 is produced. The thickness varies slightly and gradually from 4 to 20 min of oxidation. There are Mn-Cr spinels mixed with the chromium oxide. The most external part is strongly enriched in Mn and Fe in a spinel structure. The diffusivity of chromium is regarded as the main cause of the difference of oxidation behavior. In both cases, the first step is a very thin chromium oxide layer. When the oxidation conditions becomes too strong in terms of exposure time or water vapor partial pressure, this oxide layer breaks. The ferritic steel is able to heal and thicken its protective chromium oxide, preventing the breakaway. The healing would be due to the high diffusivity of chromium. The thickening would be caused by the presence of the Mn-Cr spinels which are a less effective diffusion barrier. The lower diffusivity of chromium in austenite promotes the breakaway.

Peer-review under responsibility of the Scientific Committee of SAM–CONAMET 2014

Keywords: stainless steel – oxidation - water vapor - high temperature - short terms

* Corresponding author.
E-mail address: valentin.badin@mines-paristech.fr

Peer-review under responsibility of the Scientific Committee of SAM–CONAMET 2014
doi:10.1016/j.mspro.2015.04.006

1. Introduction

AISI 441/DIN 1.4509 is a ferritic stainless steel stabilized with Nb and Ti and AISI 316L/DIN 1.4404 is an austenitic stainless steel. These alloys are often used for their strong oxidation resistance. They are widely studied at lower temperature for the nuclear industry, and studied consistently at 1100 °C for corrosion resistance during the hot rolling and annealing process [Saunders et al. (2008)]. However, most studies present variations from one to another because of the sensibility of these alloys depending on oxidation parameters. Indeed, temperature, water vapor and exposure time all have a strong impact on oxides scale. This study gives therefore a consistent look at the oxides generated in this range of parameters using complementary analysis techniques..

Regarded as essentially composed of Cr_2O_3 on the ferritic alloy, the thick oxide generated is actually more complex. An effort has been then made to identify elements, phases and their localization. If silicon oxides are known for a long time [Saunders et al. (2008)], Mn-spinels are often depicted differently [Brady et al. (2008)]. The oxides on the austenitic steel are also analysed in detail as variations have been observed depending on the water content in the atmosphere.

The study was originally aimed at a process which requires as a first step to obtain rapidly a thick and homogeneous oxide. It was therefore approached at first from the opposite aim of preventing corrosion. The results are, however, still of interest for annealing and hot rolling process investigations.

2. Experimental methods and materials

The composition of 441 and 316L stainless steels are shown in table 1. The average grain size is 40 µm for the ferritic steel and 17 µm for austenitic steel. Samples were received as skin-pass finish and cut in pieces of dimension 20x80x1 mm. Before treatment they were cleaned with acetone. The oxidation stage was performed in a belt furnace in which duration, atmosphere and temperature were set accordingly. The oxidizing atmosphere was produced from an argon flow of 0.3, 0.6 and 0.9 m^3/h passing through a water tank set at 85 °C and then mixed with 3m^3/h of pure argon. 5%, 9% and 13% of humidity was therefore obtained. Raman micro spectroscopy has been operated with an Ar^+ laser. The wavelength is 514 nm. XRD experiments are realized on a Philips X'Pert Pro MPD. X-Ray radiation is Cu-K_α. Grazing angles have been used to consider oxides rather than the bulk. 0.2 ° and 1 ° have been selected. EDS and SEM pictures were realized on a Philips XL30. XPS system is a Thermo-Fisher K-Alpha with an Al K_α source.

Table 1 – Chemical compositions (wt. %).

Grades	1.4509 / 441	1.4404 / 316L
C	0.02	≤ 0.03
Si	≤ 1	≤ 1
Mn	≤ 1	≤ 2
Cr	17.5-18.5	17-19
Mo	-	2-2.5
Ni	-	10-13
P	≤ 0.04	≤ 0.05
S	≤ 0.03	≤ 0.03
Ti + Nb	0.6	-
N	-	≤ 0.03
Fe	Bal.	Bal.

3. Results and discussion

For 2.5 min of oxidation on 441 stainless steel, a very thin nano-scale layer of protective chromium oxide is formed. For all longer exposure times until 20 min, an almost homogeneous and much thicker layer, mainly consisting of Cr_2O_3, is produced. The thickness varies slightly and gradually from 4 to 20 min of oxidation (fig. 1) as well as from 5% to 13% of H_2O (fig. 2). The range of variation goes from 2 µm to 5 µm. In other terms, the kinetic of oxidation change drastically after 2.5 min of exposure time to reach a thicker oxide steadily developed. After this point, all samples present very similar oxides. Fig. 3 presents the Raman spectrum of the surface of the

sample and from the cross-section. Both areas are spotted in the optical view. There are Mn-Cr spinels mixed with the chromium oxide in the main layer (area 2). XRD results (fig. 4) indicate a decreased ratio of the spinel phase over corundum phase from 0.2 ° to 1 ° grazing angle. XPS and EDS (fig. 5) also confirm the presence of Fe and the increase of Mn in this outer part. Coupled with Raman results, the most external part of the oxides is thus a mix of Mn, Fe and Cr spinels. The presence of a layer of SiO_2 between the bulk and chromium oxide is also visible on fig. 5.

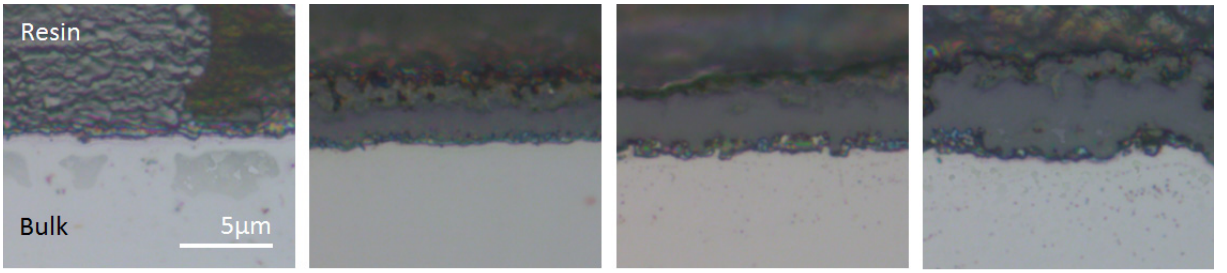

Figure 1 - 441 alloy. Optical view of cross-sections. Influence of time with constant %H_2O.

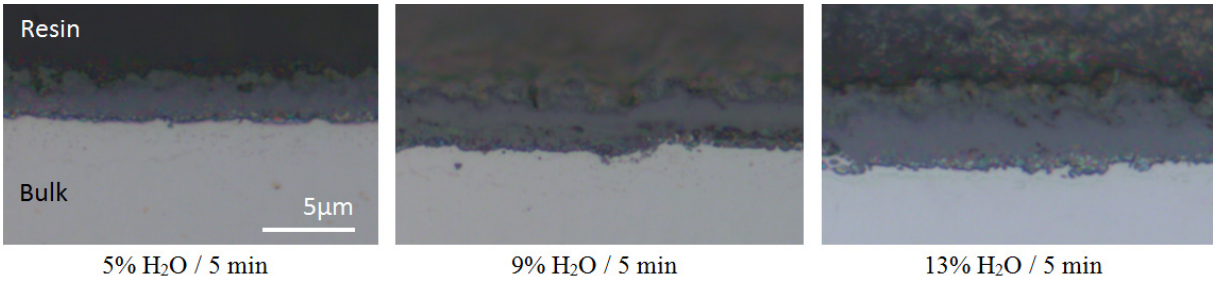

Figure 2: 441 alloy. Optical view of cross-sections. Influence of %H_2O with constant time.

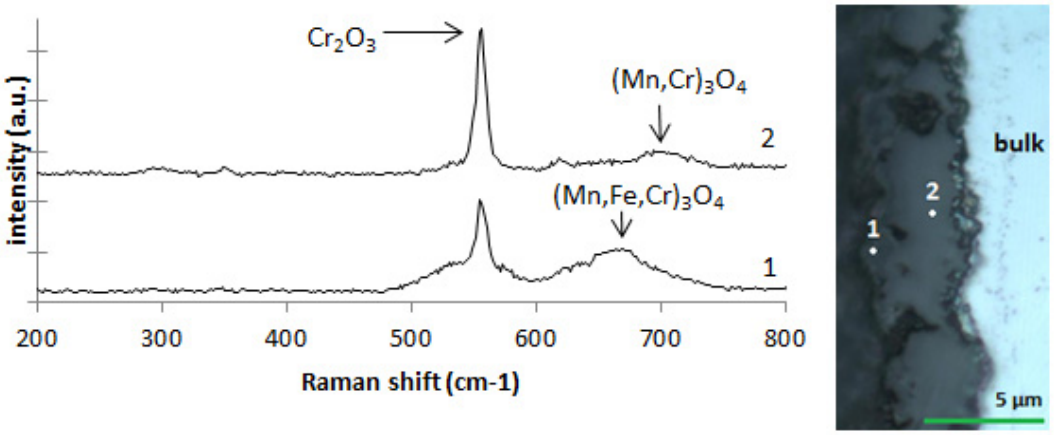

Figure 3: 441 alloy. Raman spectrum for sample Ar + 13% H_2O and 10 min. (1) top layer (2) main layer with corresponding optical view of the cross-section.

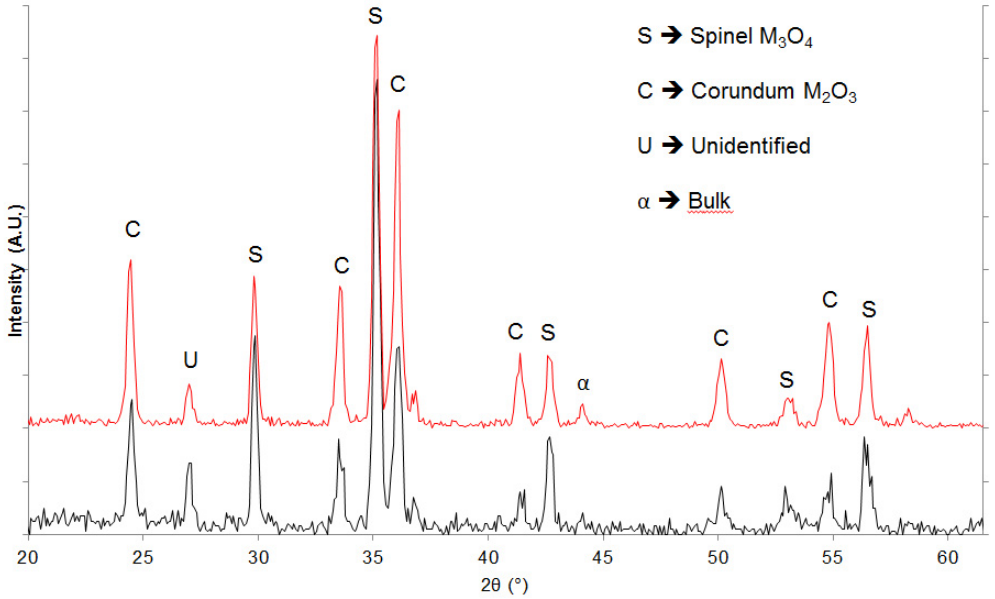

Figure 4: 441 alloy. Sample Ar + 13% H_2O and 10 min. XRD spectra for 0.2 ° and 1 ° degree of grazing incidence.

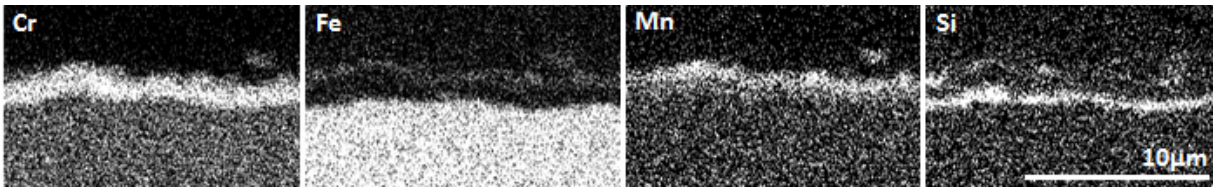

Figure 5: 441 alloy. EDS map for cross-section of sample 9% H_2O and 20

For all exposure times, 316L forms a thick oxide scale with iron oxides on its outer part and spinels for its inner part. Iron oxides are differentiated on fig. 6. For Ar + 5% H_2O, iron oxides for all durations are constituted of a single layer of wüstite $Fe_{1-x}O$. For Ar + 9% H_2O and Ar + 13% H_2O, iron oxides are systematically constituted of a layer of hematite Fe_2O_3 over a layer of magnetite slightly enriched in chromium $Fe_{3-x}Cr_xO_4$. The lower oxidizing strength of the atmosphere for 5% H_2O may be the cause of this observation as the oxide state of Fe in FeO is lower. Due to these strong oxidation conditions, oxide scale is not always homogeneous and iron oxides spallation may occur. It is true in particular for longer oxidation time and higher water vapor content. The inner oxide, confirmed by Raman (fig. 6. area 3) and EDS is always composed of a mix of mainly Fe and Cr with additions of Ni in a spinel structure.

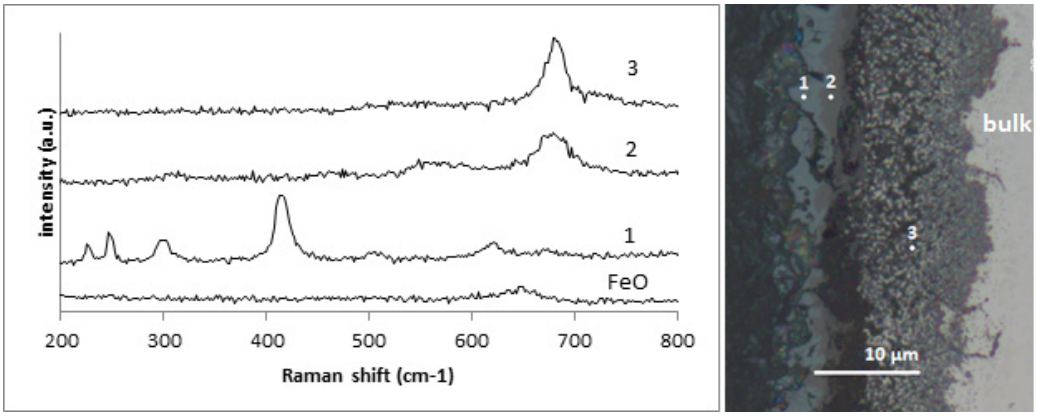

Figure 6: 316L alloy. Raman spectrum for sample Ar + 9% H_2O and 5 min with corresponding optical view of the cross-section. Peaks correspond to: (1) Fe_2O_3 (2) Fe_3O_4 (3) Mn-Cr-Ni spinel. Spectrum of FeO from sample Ar + 5% H_2O and 5 min.

The amount of chromium in a stainless steel alloy is regarded as the main factor to increase the resistance to corrosion [Lacombe et al. 1993]. In these two alloys, this amount is very similar. Their oxide layers for the parameters studied here are however very distinct. For 316L steel, the mechanism involved is called 'breakaway'. This configuration of oxides has been well studied but is not fully understood yet [Saunders et al. (2008)]. The very thin, nano-scale, chromium oxide existing at room temperature, breaks when the oxidation parameters become too strong in terms of temperature, duration or atmosphere. Several mechanisms are suggested to be involved [Saunders et al. (2008), Gheno et al. (2012), Saeki et al. (2012)]. The early layer formed is partially not adhesive and when the oxidizing molecules reach the chromium depleted bulk, the oxidation becomes steep. The significant augmentation of the diffusivity with temperature and the evaporation of chromium oxides are also considered responsible for the resulting oxides. But all of these reasons come from a lack of chromium reaching the surface to heal the defective former protective layer. Instead, it results in the use of iron as iron oxides and Fe-spinels, both present in the breakaway oxides. Yet, the main difference between austenitic and ferritic steels is the structure given by the presence or the absence of Ni. At high temperature, the diffusivity of chromium is higher in the ferritic lattice [Peraldi and Pint (2004)]. This difference of diffusivity is therefore regarded as the main cause of the difference of oxidation behavior between the two grades. When the initial protective layer is unable to prevent the oxidizing of the ferritic alloy, enough chromium reaches the surface for the parameters used in this study. Indeed, ferritic stainless steels can also have a breakaway oxidation mechanism usually for longer durations or weaker alloys [Brady et al. (2008), Gheno et al. (2012), Saeki et al. (2012), Peraldi and Pint (2004)]. Si and Mn have been found to be essential in this range of treatment durations to avoid the breakaway [Ledoux et al. (2013), Gonzales et al. (2008)]. The formation of Mn-spinels onto the external layer limits the chromium oxide evaporation and the SiO_2 layer acts as a diffusion barrier. However, their presence in the ferritic alloy and their role in the oxidation do not justify the difference with the 316L as they are present in both grades. The grain size does not justify the difference in behavior either as grain size in 441 alloy is bigger than in 316L alloy.

4. Conclusion

Ferritic stainless steel 441 has a better corrosion resistance for the parameters studied. After 2.5 min of oxidation, it always results in a few microns thick main layer of Cr_2O_3 mixed with $(Mn,Cr)_3O_4$. More spinel phase, with Fe, Mn and Cr are present on the outer part. A thin layer of SiO_2 forms a barrier with the bulk. 316L alloy presents in all cases a breakaway type oxide scale. The amount of water vapor plays a role in the nature of the iron oxides formed on the outer part. FeO is observed for lower water vapor partial pressure and both Fe_2O_3 and Fe_3O_4 are present for higher water vapor content. Inner oxides are constituted of Fe-Cr-Ni spinels. The higher diffusivity of chromium in the ferritic lattice plays a major role by modifying the oxidation mechanism and thus, the oxides scale. As a result

from the original purpose of this work stated in the introduction, both grades produce a thick oxide. 441 Alloy is however more homogeneous without spallation issues.

Acknowledgements

This research is financed by Linde AG. The scientific and technical help of L. Bellot-Gurlet, S. Jacomet and G. Monge was sincerely appreciated.

References

Brady M.P., Keiser J.R., More K.L., Fayek M., Walker L.R., Peascoe-Meisner R.A., Anovitz L.M., Wesolowski D.J., Cole D.R., 2008. Comparison of Short-Term Oxidation Behavior of Model and Commercial Chromia-Forming Ferritic Stainless Steels in Dry and Wet Air. Oxidation of Metals 78, 1–16

Gheno T., Monceau D., Young D.J. , 2012. Mechanism of breakaway oxidation of Fe–Cr and Fe–Cr–Ni alloys in dry and wet carbon dioxide. Corrosion Science 64, 222–233

Gonzales S., Combarmond L., Tran M.T., Wouters Y., Galerie A. , 2008. Short Term Oxidation of Stainless Steels during Final Annealing. Materials Science Forum Vols. 595-598, 601-610

Lacombe P., Baroux B., Béranger G., 1993. Stainless steels. Les Ulis, France, Les éditions de physiques

Ledoux X., Mathieu S., Vilasi M. , Wouters Y. , Del-Gallo P. , Wagner M. , 2013. Oxide Growth Characterization During Short-Time Oxidation of a Commercially Available Chromia-Forming Alloy (HR-120) in Air at 1,050°C. Oxidation of Metals 80, 25–35

Peraldi R. , Pint B.A., 2004. Effect of Cr and Ni Contents on the Oxidation Behavior of Ferritic and Austenitic Model Alloys in Air with Water Vapor. Oxidation of Metals 61, Nos. 5/6

Saeki I., Sugiyama Y. , Hayashi S., Yamauchi A. , Doi T. , Nishiyama Y. , Kyo S. , Suzuki S. , Sato M. , Fujimoto S. , 2012. In situ X-ray diffraction of surface oxide on type 430 stainless steel in breakaway condition using synchrotron radiation. Corrosion Science 55, 219–225

Saunders S.R.J., Monteiro M. , Rizzo F. , 2008. The oxidation behavior of metals and alloys at high temperatures in atmospheres containing water vapor: A review. Progress in Materials Science 53, 775–837